RESEARCH ARTICLE

Development of a reverse genetics system for Sosuga virus allows rapid screening of antiviral compounds

Stephen R. Welch, Ayan K. Chakrabarti, Lisa Wiggleton Guerrero, Harley M. Jenks, Michael K. Lo, Stuart T. Nichol, Christina F. Spiropoulou, César G. Albariño*

Viral Special Pathogens Branch, Division of High-Consequence Pathogens and Pathology, National Center for Emerging and Zoonotic Infectious Diseases, Centers for Disease Control and Prevention, Atlanta, GA, United States of America

* calbarino@cdc.gov

Check for updates

Abstract

Sosuga virus (SOSV) is a recently discovered zoonotic paramyxovirus isolated from a single human case in 2012; it has been ecologically and epidemiologically associated with transmission by the Egyptian rousette bat (*Rousettus aegyptiacus*). Bats have long been recognized as sources of novel zoonotic pathogens, including highly lethal paramyxoviruses like Nipah virus (NiV) and Hendra virus (HeV). The ability of SOSV to cause severe human disease supports the need for studies on SOSV pathogenesis to better understand the potential impact of this virus and to identify effective treatments. Here we describe a reverse genetics system for SOSV comprising a minigenome-based assay and a replication-competent infectious recombinant reporter SOSV that expresses the fluorescent protein ZsGreen1 in infected cells. First, we used the minigenome assay to rapidly screen for compounds inhibiting SOSV replication at biosafety level 2 (BSL-2). The antiviral activity of candidate compounds was then tested against authentic viral replication using the reporter SOSV at BSL-3. We identified several compounds with anti-SOSV activity, several of which also inhibit NiV and HeV. Alongside its utility in screening for potential SOSV therapeutics, the reverse genetics system described here is a powerful tool for analyzing mechanisms of SOSV pathogenesis, which will facilitate our understanding of how to combat the potential public health threats posed by emerging bat-borne paramyxoviruses.

Author summary

Shortly after returning from a field trip to South Sudan and Uganda in 2012, a wildlife researcher presented to the emergency room with high fever and muscle and joint pain, that later progressed to severe disease. Sosuga virus (SOSV), a novel paramyxovirus, was identified as the etiological agent. Further epidemiological investigations identified bats as the probable reservoir of SOSV. Other related bat-borne paramyxoviruses, such as Nipah and Hendra viruses, have developed into major public health issues, raising concern that SOSV could represent an emerging threat. We developed a SOSV reverse genetics system

to screen antiviral compounds and identify putative therapeutic interventions. Using this system, we generated a reporter virus capable of expressing a fluorescent protein in infected cells. By incorporating the reporter SOSV into a high-throughput screening assay, we identified several compounds that inhibit SOSV replication. In addition to antiviral screening, this rescue system can be used to investigate disease mechanisms, and to contribute to development of public health interventions for threats posed by emerging bat-transmitted paramyxoviruses.

Introduction

The Paramyxoviridae (order *Mononegavirales*) represent a diverse family of viruses, many of which, such as measles virus, respiratory syncytial virus, and mumps virus, are significant human pathogens [1]. Within this family, bat-borne paramyxoviruses have previously been recognized as potential novel zoonotics with the ability to spill over into the human population and cause disease [2–4]. The 2 bat-transmitted paramyxoviruses with the greatest public health impact to date are Hendra (HeV) and Nipah (NiV) viruses, which together comprise the *Henipavirus* genus and are vectored by fruit bats of the *Pteropus* genus [5]. First recognized in 1994, HeV infections in both domestic horses and humans have occurred sporadically [6,7], while NiV infections in Bangladesh, India, and Malaysia have resulted in over 600 human infections to date [8].

Sosuga virus (SOSV) is a recently discovered zoonotic paramyxovirus [9]. It was first identified from a single clinical case in 2012, when a wildlife researcher who conducted a 6-week field expedition in South Sudan and Uganda presented with fever, generalized myalgia and arthralgia, neck stiffness, and a sore throat shortly upon returning to the USA [10]. The patient was hospitalized as symptoms worsened, including the development of a confluent maculo-papular rash; after 14 days, all symptoms had sufficiently resolved to allow discharge. After several differential diagnoses were ruled out, sequence analysis revealed the presence of a novel rubula-like paramyxovirus in samples taken from the patient, from which the virus was later isolated. Further ecological and epidemiological investigations revealed Egyptian rousette bats (*Rousettus aegyptiacus*) as the likely reservoir for the virus, with this case representing a single spillover event into humans [11]. While only one case of SOSV infection has been confirmed to date, its detection in bat populations sampled over a 3-year period at multiple geographic locations in Uganda means that the possibility exists for future spillover events into the human population [11].

Reverse genetics systems allow for precise manipulation of viral genomes, and the ability to modify them to suit the required application. One such application is the generation of recombinant viruses expressing reporter proteins that facilitate indirect quantification of viral replication in infected cells. However, for pathogenic viruses such as SOSV, which require manipulation under high biocontainment levels, minigenome-based assays are also valuable surrogates that recapitulate viral replication and transcriptional processes without generating infectious particles. Here we describe a reverse genetics system for SOSV that can be used to rapidly screen for compounds that inhibit viral replication. An initial minigenome screen performed under biosafety level 2 (BSL-2) biocontainment was used to identify only those compounds with potential antiviral activity, which were then assessed for their ability to inhibit authentic viral replication processes using the reporter SOSV at BSL-3. As well as screening for antiviral compounds, these reverse genetics system will provide a powerful tool for analyzing mechanisms of SOSV pathogenesis in both in vitro and in vivo systems.

Materials and methods

Cells

Huh7 cells (ATCC, USA) were cultured in Dulbecco's modified Eagle's medium (DMEM) supplemented with 5% (v/v) fetal calf serum, non-essential amino acids, 100 U/mL penicillin, and 100 µg/mL streptomycin. BSR-T7/5 (generous gifts from Klaus Conzelmann, Germany), BHK-1 (ATCC, USA), and Vero-E6 cells (ATCC, USA) were cultured in DMEM supplemented with 10% (v/v) fetal calf serum, non-essential amino acids, 1 mM sodium pyruvate, 2 mM L-glutamine, 100 U/mL penicillin, and 100 µg/mL streptomycin.

Reverse genetics: Minigenome assay and rescue of recombinant viruses

The SOSV minigenome segment was cloned into a Pol-I promoter-based plasmid (S1 Fig., Genbank #MG880223), and transfected into Huh7 cells in conjunction with Pol-II expression plasmids (pCAGGS) supplying SOSV polymerase (L), nucleoprotein (NP), and phosphoprotein (P) proteins in trans. The minigenome assay was performed in a 96-well plate on cells seeded at 2×10^4 cells per well, with the following amounts of plasmids (150 ng total) transfected per well: 75 ng minigenome, 12.5 ng L, 50 ng NP, and 12.5 ng P. Minigenome activity was based on ZsGreen1 (ZsG) fluorescence levels determined at 72 h post transfection (hpt). To rescue recombinant virus, a T7 promoter-based plasmid containing full-length anti-genomic sense SOSV (S2 Fig.; Genbank #MG880224) was constructed. To rescue the reporter SOSV expressing ZsG, a modified genome was constructed in which the M open reading frame (ORF) was replaced with one encoding ZsG-P2A-M, leaving the M gene start and gene end intact (S2 Fig.; Genbank #MG880225). Virus rescue was performed in 6-well plates seeded with BSR-T7 cells (approximately 70% confluent) transfected with genome plasmid in conjunction with the SOSV-L, -NP, and -P expression plasmids (2 µg genome, 1 µg SOSV-L, 0.5 µg SOSV-NP, and 0.25 µg SOSV-P). At 96 hpt, cell culture supernatants were harvested, clarified by low-speed centrifugation, and used to infect BHK-21 cells. At 96 h post infection (hpi), cell culture supernatants were harvested, clarified, and titered by tissue culture infective dose 50 ($TCID_{50}$) assays in Vero-E6 cells based on crystal violet visualization of cytopathic effects [12].

Antiviral compound screening

All compounds were obtained from either Selleckchem (Houston, TX, USA) or Sigma-Aldrich (Saint Louis, MO, USA) with the exception of T-705 (BOC Sciences, Shirley, NY, USA) and 09167 (Vitas-M Laboratory, Champaign, IL, USA). For both screening assays, Huh7 cells were seeded in a 96-well plate at 2×10^4 cells per well 16–20 h prior to treatment with DMSO-diluted compounds (final DMSO concentration 0.5%). For the minigenome screening assay, cells were transfected with the required plasmids using TransIT- LT-1 (Mirus Bio, Madison, WI, USA) 1 h post treatment. Total ZsG fluorescence was determined 72 hpt using a microplate reader (H1MD, BioTek Synergy, Winooski, VT, USA), with levels recorded at a height of 6 mm with 75 gain/sensitivity. ZsG levels were normalized to levels in mock-treated cells. For the reporter and wild-type screening assays, cells were infected 1 h post treatment with either rSOSV/ZsG or rSOSV at MOI 0.2. At 48 hpi, supernatants were collected (rSOSV-infected cells) for titer determination, or total ZsG fluorescence in the infected cell monolayer determined (rSOSV/ZsG-infected cells) using a H1MD plate reader (height 6 mm; 100 gain/sensitivity). For both assays, cell viability was determined by measuring ATP content in parallel with compound-treated, mock-transfected/infected cells using CellTiter-Glo 2.0 (Promega, Madison, WI, USA). All experiments were performed in quadruplicate and repeated at least 3 times.

Microscopy and high-content imaging

ZsG fluorescence in infected cells was imaged directly using an EVOS digital inverted microscope (Thermo-Fisher, Waltham, MA, USA). For immunofluorescence, cells were fixed in 10% formalin for 30 min, permeabilized in PBS containing 0.1% Triton-X100 (v/v) for 10 min, and blocked with PBS 5% BSA (v/v) for 30 min. Primary antibody was rabbit α-SOSV NP (Genscript, Waltham, MA, USA), visualized with an AlexaFluor 488-labeled secondary antibody (Thermo-Fisher, #A11034). Quantification of total rSOSV protein production in Huh7 cells was performed on infected cells labeled as described above, and further stained with Nuc-Blue and Cell-Mask Red (Thermo-Fisher). Images were collected on the Operetta high-content imaging system (PerkinElmer, Waltham, MA, USA) using a 20× objective, with 16 fields per well analyzed using the Harmony software package (PerkinElmer). Total 488 fluorescence per field was determined, averaged for the well, and then normalized to values from control wells containing rSOSV-infected, mock-treated cells.

Data analysis

ZsG fluorescence values for compound-treated, rSOSV/ZsG-infected cells were normalized to those in mock-treated (DMSO only) cells, and used to fit a 4-parameter equation to semilog plots of the concentration-response data. From this, the compound concentrations inhibiting 50% of the ZsG expression (50% effective concentration, EC_{50}) were interpolated. Cell viability was similarly calculated in compound-treated, mock-infected cells to determine the 50% cell cytotoxicity concentration (CC_{50}) of each compound. The selectivity index (SI) was calculated by dividing the CC_{50} by the EC_{50}. Data analysis was performed using GraphPad Prism v7. Suitability for high-throughput screening was determined using the Z prime (Z′) score, a measure of statistical effect size, with values between 0.5 and 1.0 considered acceptable [13].

Accession numbers

SOSV Minigenome plasmid; pSOSV MG; Genbank # MG880223
   Rescue plasmid for rSOSV; pSOSV FL; Genbank #MG880224
   Rescue plasmid for rSOSV/ZsG; pSOSV/ZsG FL, Genbank #MG880225

Results

Screening of antiviral compounds using a SOSV minigenome assay

We constructed a SOSV minigenome segment containing the parental SOSV 3′ and 5′ leader and trailer sequences, along with the gene start sequence for NP and the gene end sequence for L. All internal coding sequences and intergenic regions were replaced with the coding sequence for ZsGreen1 (ZsG), a green fluorescent protein (Fig 1A). Protein expression plasmids under control of the Pol-II promoter (pCAGGS) allowed in trans expression of SOSV NP, L, and P, the minimum requirement to initiate paramyxovirus replication and transcription [1]. The minigenome segment was cloned into a Pol-I expression plasmid in the negative orientation, meaning it has to be replicated first by the NP + L + P replication complex before transcription of ZsG mRNA can occur.

Next, the SOSV minigenome screen was optimized to achieve maximum reporter protein expression with the greatest signal-to-noise ratio in a 96-well plate format using Huh7 cells. Huh7 cells have previously proven useful for evaluating nucleoside analog activity against other viruses, and are highly permissive to SOSV infection [14–17]. Alongside a constant amount of minigenome plasmid, differing ratios of pCAGGS-L, -NP, and -P were transfected, and ZsG fluorescence was determined at both 48 and 72 hpt (Fig 1B). We determined the
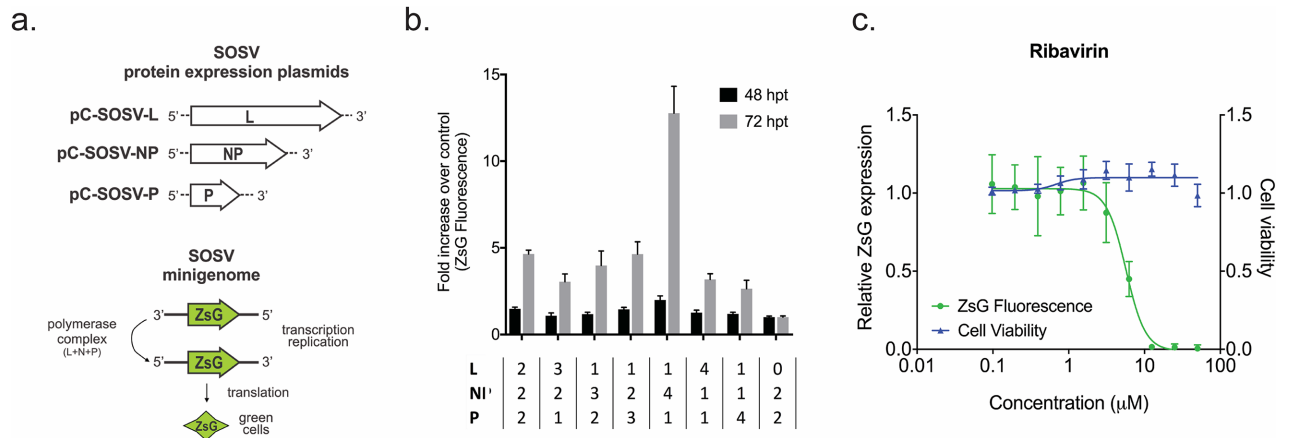
Fig 1. Design and optimization of the Sosuga virus minigenome screening assay. a. Genome schematic representing the design of the Sosuga virus (SOSV) minigenome segment. The minigenome contains the full-length SOSV 3′ and 5′ leader and trailer sequences, along with the gene start sequence for nucleoprotein (NP) and the gene end sequence for the viral polymerase (L), with the parental coding and intergenic regions replaced by the coding sequence of ZsGreen1 (ZsG). Transfected into cells in conjunction with plasmids expressing SOSV L, NP, and phosphoprotein (P), this minigenome allows for expression of quantifiable ZsG. **b.** The minigenome assay was optimized for Huh7 cells in a 96-well plate format using different ratios of the plasmids expressing L, NP, and P with a constant amount of minigenome plasmid. Cells were transfected with 75 ng minigenome plasmid and 75 ng total of plasmids expressing L, NP, and P, with ratios of each stated underneath the bars. Relative ZsG fluorescence over control reactions with no L was calculated at 48 and 72 h post transfection (hpt). **c.** Dose-response curve for the optimized SOSV minigenome assay against ribavirin. Cells were treated with a serial 2-fold dilution of ribavirin 1 hpt with the minigenome plasmids, and ZsG fluorescence was measured at 72 hpt. ZsG fluorescence (green) was normalized to mock-treated cells (DMSO only). Cell viability (blue) was determined concurrently by measuring ATP content, with values normalized to mock-transfected cells. Each point represents the mean of quadruplicate wells, with error bars showing standard deviation; graph is representative of 3 independent experiments.

optimal ratio of plasmids for the assay to be 6:1:4:1 of genome, pCAGGS-L, -NP, and–P respectively, with ZsG fluorescence read at 72 hpt. To determine whether the optimized minigenome assay was suitable for screening antiviral compounds, we used the broad-spectrum antiviral ribavirin. Using 50 μM ribavirin as the positive control and DMSO as the vehicle-only control, the Z′ score of the assay was 0.58. Dose-dependent reduction of ZsG fluorescence was also observed in the SOSV minigenome assay using a serial 2-fold dilution of ribavirin, giving an EC_{50} of 5.91 ± 0.85 μM with no cytotoxicity ($CC_{50} > 50$ μM; Fig 1C). These data indicated that the assay was robust, and suitable for screening anti-SOSV compounds at BSL-2.

As minigenome assays can be used as surrogates for measuring viral replication and transcription, we evaluated a panel of 40 compounds predicted to inhibit these processes. These were a collection of nucleoside analogs supplemented with other select compounds reported to inhibit viral replication. Compounds were initially screened for activity at concentrations of 5000, 500, and 50 nM, with cell viability determined concurrently by assessing ATP content (S1 Table). Compounds inhibiting the minigenome by >50% whilst retaining >80% cell viability were then chosen for further analysis; these were 2′-deoxy-2′-fluorocytidine (2′-dFC), 5-fluorouridine, mycophenolic acid (MPA), and 6-azauridine. Dose-response analysis of these compounds demonstrated that both 2′-dFC and 6-azauridine inhibited minigenome activity in the absence of cell toxicity, with EC_{50} values of 1.31 ± 0.15 μM and 5.17 ± 1.01 μM, respectively (Fig 2). While 5-fluorouridine was not cytotoxic at the concentrations evaluated, it did not completely inhibit minigenome signal even at the highest concentrations evaluated, and was therefore dropped at this point. MPA inhibited minigenome activity at sub-micromolar concentrations, but was cytotoxic at higher concentrations. However, with an SI of 7, it was incorporated into the secondary virus screen to determine if a larger therapeutic window became apparent in the context of authentic viral replication.
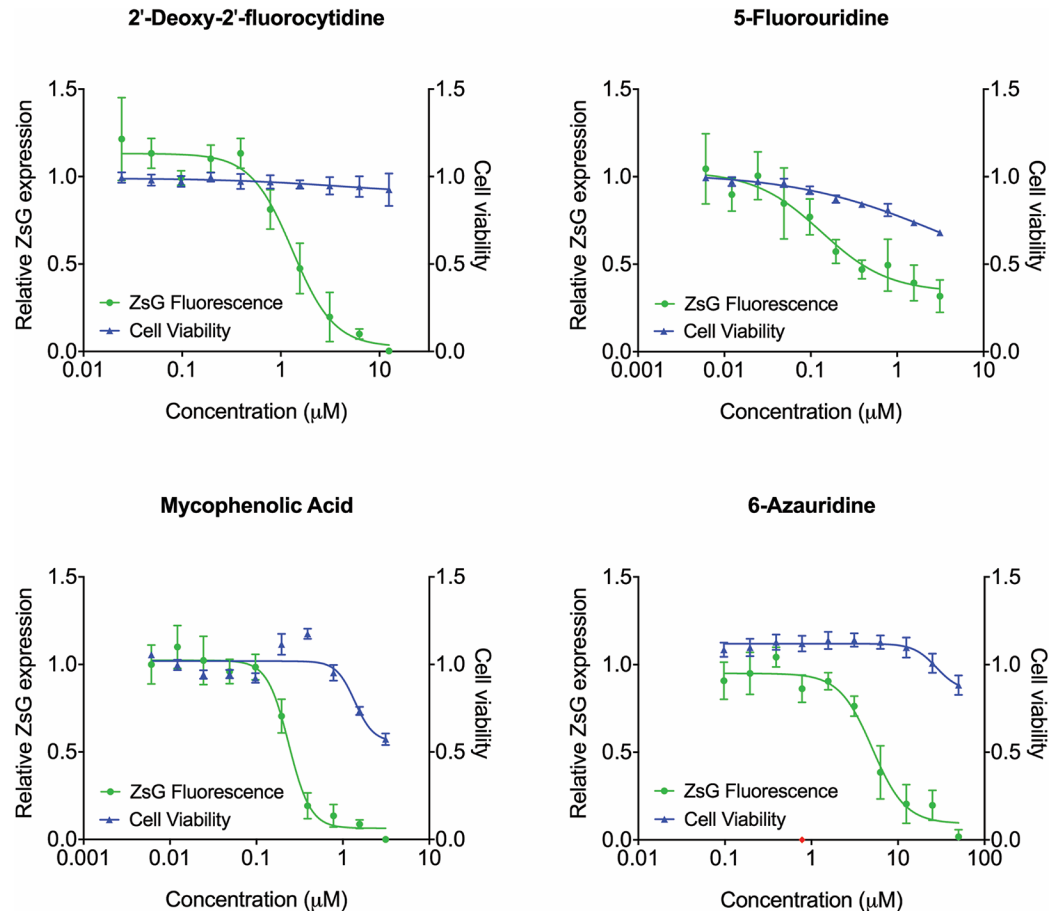
Fig 2. Dose-response curves for selected compounds using the minigenome assay. Compounds selected during the initial screen as potential SOSV antivirals were assessed by concentration-response curves using serial 2-fold dilutions of each compound. ZsG fluorescence (green) at 48 hpt was normalized to levels in mock-treated cells (DMSO only). Cell viability (blue) was determined concurrently by measuring ATP content, with values normalized to those in mock-transfected cells. Graphs are representative of at least 3 independent experiments. Each point represents the mean of quadruplicate wells, with errors bars indicating the standard deviation.

https://doi.org/10.1371/journal.pntd.0006326.g002

Design and rescue of a reporter SOSV expressing a fluorescent protein

The single-stranded, negative-sense RNA genome of SOSV encodes 6 genes to express 7 proteins, with 1 protein generated by V/P gene mRNA editing. The intergenic regions of SOSV contain transcriptional promoter and terminator sequences. We cloned the full-length SOSV genome into an expression plasmid under control of the T7 polymerase promoter. When transfected into cells and supplied with SOSV P, NP, L, and T7 polymerase in trans, this system successfully generated infectious recombinant SOSV (rSOSV). After optimizing the rSOSV rescue system, we designed another recombinant SOSV genome capable of expressing a fluorescent reporter protein in infected cells. Previous approaches to develop recombinant paramyxoviruses expressing reporter genes have included the reporter as either a separate open reading frame (ORF), or incorporated it within a parental ORF [18–22]. We employed the latter approach, and generated a SOSV genome in which the ZsG ORF was inserted upstream of the M ORF, fused to the viral protein via the self-cleaving P2A motif taken from porcine teschovirus 1 [23]. The authentic SOSV M gene start and gene end sequences therefore transcribe a single mRNA encoding the ORF for both M and ZsG, which, upon translation, results
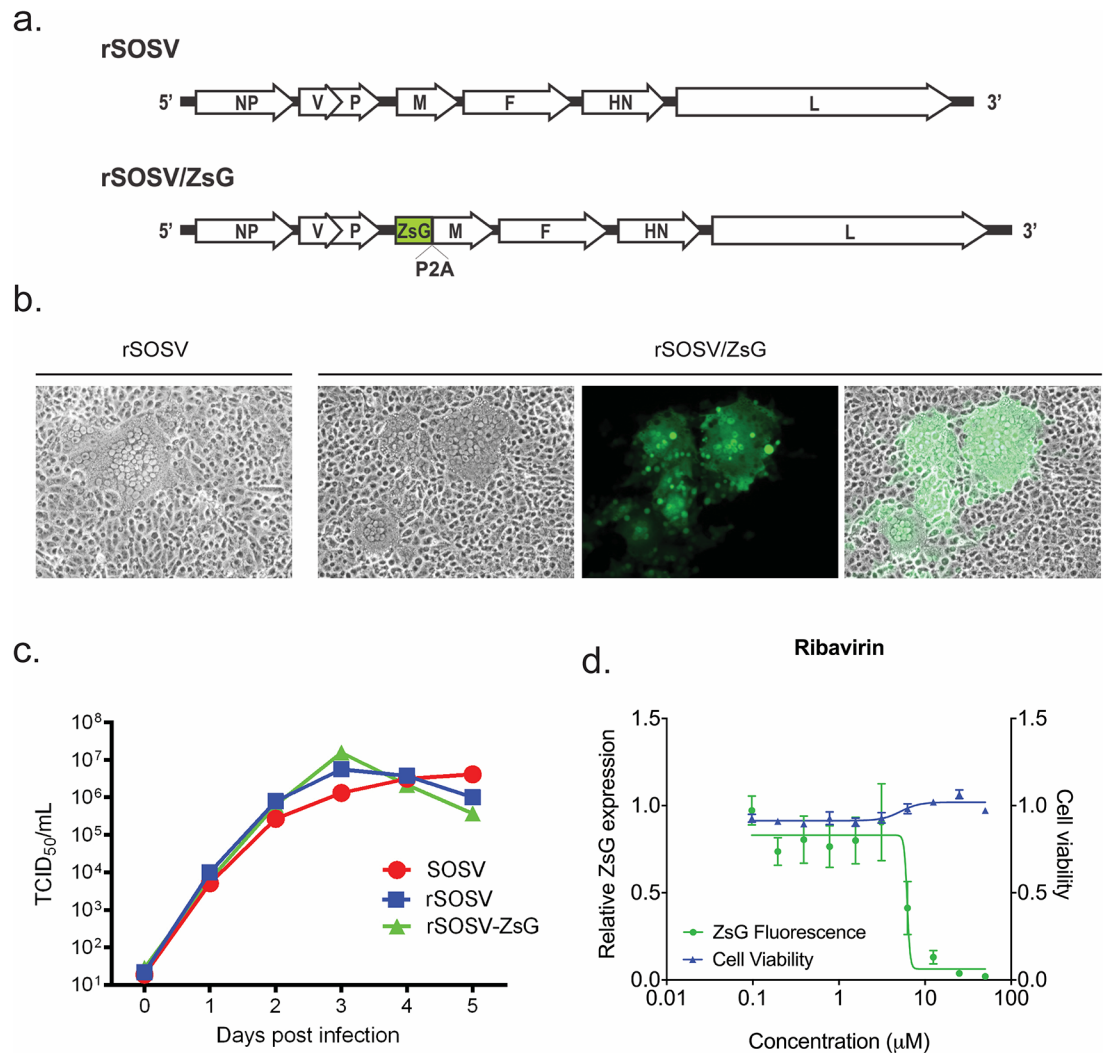
Fig 3. Optimization of an antiviral screening assay using a recombinant SOSV expressing ZsG. a. Schematic representation of the wild-type recombinant SOSV (rSOSV), and the reporter SOSV expressing ZsG (rSOSV/ZsG). The ZsG coding sequence was inserted immediately 5′ of the M coding sequence (antigenomic sense), separated from the viral protein by the P2A sequence from porcine teschovirus 1. This self-cleaving amino acid motif allows expression of both ZsG and M from a single mRNA generated by the parental SOSV M promoter and terminator sequences. **b.** Vero-E6 cells infected with either rSOSV or rSOSV/ZsG at 72 hpi showing formation of syncytia. In rSOSV/ZsG-infected cell monolayers, syncytia were associated with extensive ZsG expression (images taken at 4 × magnification). **c.** Growth curves for wild-type SOSV, rSOSV, and rSOSV/ZsG were performed in Vero-E6 cells infected at MOI 0.1. Titers ($TCID_{50}$) were determined at 24, 48, 72, 96, and 120 hpi. **d.** The optimized rSOSV/ZsG antiviral screening assay was validated using ribavirin. Huh7 cells were treated with a serial 2-fold dilution of ribavirin 1 h prior to infection at MOI 0.2. ZsG fluorescence (green) was measured at 72 hpi and normalized to levels in mock-treated cells (DMSO only). Cell viability (blue) was determined concurrently by measuring ATP content, with values normalized to mock-infected cells. Each point represents the mean of quadruplicate wells, with error bars showing standard deviation; graph representative of 3 independent experiments.

in the expression of 2 separate proteins via the P2A ribosomal skipping motif. Incorporation of this recombinant SOSV genome into the previously described SOSV rescue system (Fig 3A) resulted in the successful rescue of the reporter SOSV (rSOSV/ZsG).

Infecting Vero-E6 cells with rSOSV/ZsG at MOI 0.1 resulted in extensive syncytia formation in the cell monolayer similar to infection with rSOSV, with strong ZsG fluorescence detectable in these infected cells (Fig 3B). To compare growth kinetics of the recombinant

viruses, Vero-E6 cells were infected with rSOSV, rSOSV/ZsG, or wild-type SOSV at MOI 0.1, with titers determined by $TCID_{50}$ at 24, 48, 72, 96, and 120 hpi. All 3 viruses grew to similar titers over the 120 h time course, with no attenuation apparent in either of the recombinant viruses compared to the wild-type (Fig 3C). This indicated that incorporation of the ZsG ORF into the SOSV genome did not negatively impact the virus phenotype. To assess whether rSOSV/ZsG could be used to confirm antiviral activity of a compound by measuring the reduction in ZsG fluorescence in treated cells, we optimized a screening assay in Huh7 cells using 50 μM ribavirin as the positive control; the resultant Z′ score was 0.74, indicating a robust assay. A concentration-response curve using a 2-fold serial dilution of ribavirin demonstrated dose-dependent reduction in ZsG fluorescence in rSOSV/ZsG-infected cells, giving an EC_{50} of 6.10 ± 0.09 μM with no cytotoxicity (CC_{50} > 50 μM; Fig 3D).

Screening of candidate antiviral compounds with recombinant viruses

To confirm the inhibitory effect of 2′-dFC, 6-azauridine, and MPA in the context of authentic viral replication, we performed counter-screening with rSOSV/ZsG. Alongside these 3 compounds, we included 09167, an antagonist of the innate immune system that was shown to inhibit NiV and other paramyxoviruses in a similar screening assay [22,24]. Huh7 cells were treated with compound 1 h prior to infection with rSOSV/ZsG at an MOI of 0.2, with ZsG fluorescence read 48 hpi. All 3 compounds reduced ZsG expression in a dose-dependent manner, with EC_{50} values similar to those observed during the minigenome screen (Fig 4A). 2′-dFC (EC_{50} = 1.48 ± 0.22 μM) and 6-azauridine (EC_{50} = 7.99 ± 1.32 μM) potently inhibited ZsG fluorescence without cytotoxicity at the highest compound concentrations. While MPA had an EC_{50} value of 0.33 ± 0.04 μM, similar to that obtained in the minigenome screen, it again had a low SI of 5 due to its cytotoxicity at higher concentrations (Table 1). The 0.67 ± 0.05 μM EC_{50} value of 09167 was consistent with the sub-micromolar concentrations used to inhibit other paramyxoviruses, indicating that SOSV was similarly sensitive to this compound [24].

To ensure the validity of using the ZsG-expressing virus to accurately identify specific inhibitors, we investigated whether these compounds also inhibited the replication of rSOSV. Huh7 cells were treated with 2′-dFC, 6-azauridine, MPA, or 09167, and infected with rSOSV (MOI = 0.2) 1 h post treatment. At 48 hpi, cells were fixed and total SOSV protein production was visualized using rSOSV-specific and fluorescently labelled antibodies. Total fluorescence due to rSOSV protein staining per well (average of 16 analyzed fields per well) was normalized to rSOSV-infected, mock-treated cells, allowing determination of the relative reduction in virus replication due to the inhibitory effects of each compound. All compounds tested reduced rSOSV protein production in a dose-dependent manner, indicating inhibition of viral replication and growth (Fig 4B). Direct visualization of the compound-treated rSOSV infected cell monolayers clearly demonstrated the reduction in viral protein production, and also demonstrated the ability of rSOSV to form extensive syncytia in Huh7 cells at sub-optimal concentrations of compound (Fig 5). These results indicate that inhibition caused by the compounds is indeed due to a SOSV-specific mechanism, rather than one unique to the ZsG-expressing recombinant.

Discussion

That SOSV, a previously unknown paramyxovirus vectored by bats, could cause severe disease in humans is not unexpected, given that bats are increasingly implicated as sources of novel zoonotic infections [3,25–27]. A recent study focusing on only 10% of bat species in relatively small geographic areas discovered evidence of 66 novel paramyxoviruses [28], so undiscovered pathogens with the capacity to threaten human health may yet be present in bat populations
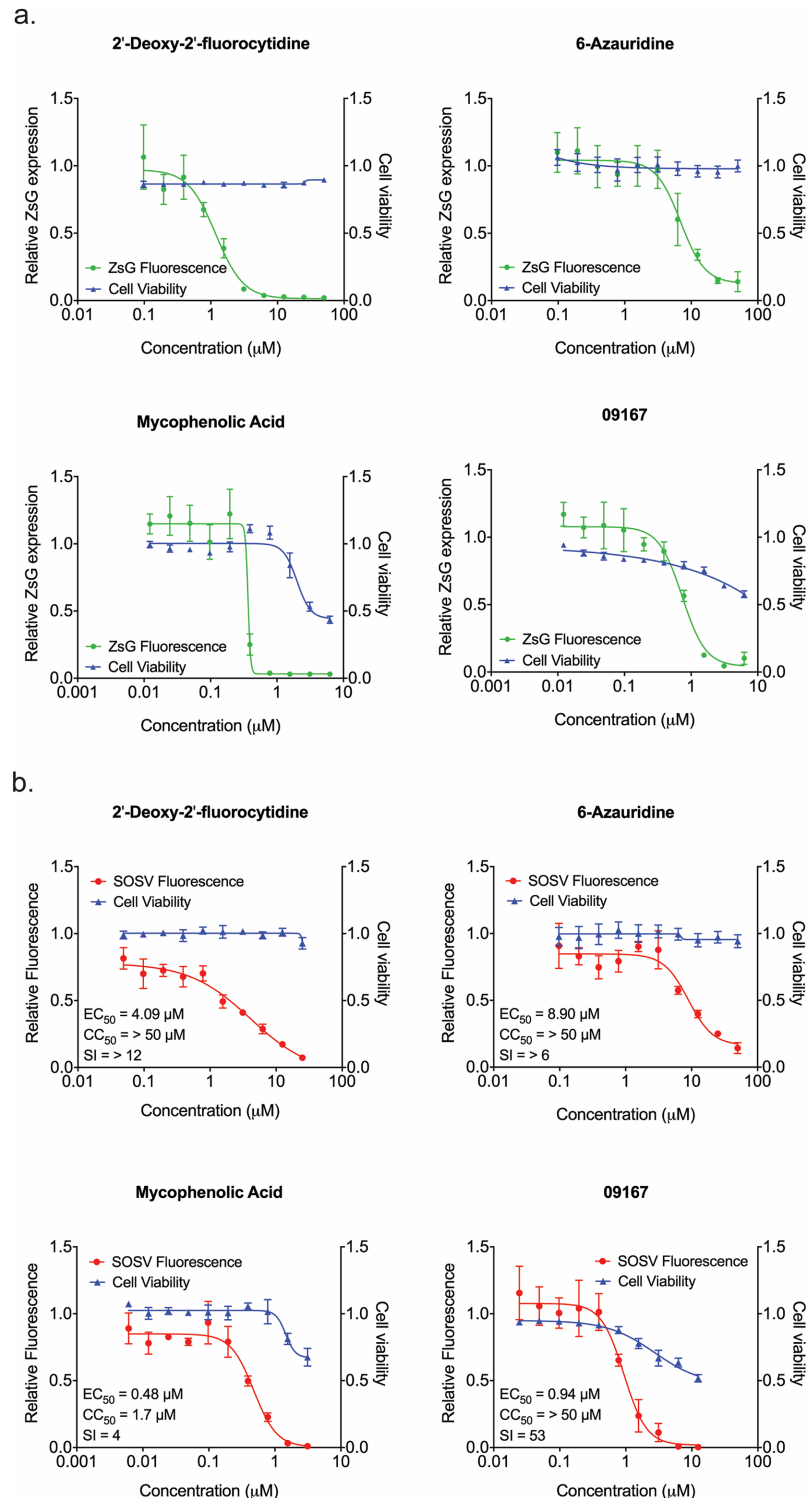
a.

b.

Fig 4. Using SOSV/ZsG as a tool to screen antiviral compounds. a. Representative concentration-response curves of Huh7 cells treated with 2-fold serial dilutions of compound 1 h prior to infection with rSOSV/ZsG at MOI 0.2. ZsG fluorescence (green) was measured at 48 hpi and normalized to mock-treated cells. Cell viability was assessed concurrently by determining ATP content (blue), with values normalized to mock-infected cells. Each point represents the mean of quadruplicate wells, with error bars showing standard deviation; graph is representative of 3 independent experiments. **b.** Confirmatory counter-screening of each compound with wild-type rSOSV. Huh7 cells were treated with serial dilutions of compound 1 h prior to infection with rSOSV at MOI 0.2. At 2 days post infection cells were

fixed, and SOSV proteins stained and quantified using immunofluorescence microscopy. Relative fluorescence (red; total fluorescence normalized to mock-treated cells) in each well was determined, with cell viability assessed concurrently by determining ATP content (blue). Each point represents the mean of quadruplicate wells, with error bars showing standard deviation. Values stated are the 50% effective concentration (EC_{50}), 50% cytotoxic concentration (CC_{50}), and selectivity index (SI).

worldwide. With reverse genetics systems already developed for the highly pathogenic paramyxoviruses NiV and HeV, the establishment of SOSV reverse genetics based on similar design concepts ensures that any investigations into future outbreaks can be quickly initiated [20,21,29]. Furthermore, a common feature of paramyxoviruses appears to be that expression of reporter genes does not negatively affect the viral phenotype either in vitro or in vivo, increasing the usefulness of these systems [21,22,30,31]. The minigenome screening methods described here were successfully used to identify several compounds that inhibit SOSV replication. We were then able to confirm the antiviral activity of candidate compounds by using the reporter virus screen. While the minigenome screen is useful for identifying compounds that inhibit viral replication and transcription, the reporter virus screen can be utilized to identify other compounds, especially those that affect other viral life cycle processes, such as cell tropism, entry, budding, and transmission.

The antiviral activity of 6-azauridine and its derivatives toward several viruses has been reported, including for viruses closely related to SOSV, such as NiV, measles, and human parainfluenza virus 3 [22,32,33]. In a clinical setting, the derivative 6-azauridine triacetate has been used therapeutically to treat severe psoriasis for over 40 years, with minimal side effects observed at a dosage level of 125 mg/kg/day [34,35]. Encouragingly, research also shows that at that dose, plasma concentrations in human subjects reach 100 μM or greater, with successive doses over several days maintaining this level [36]. This is far in excess of the 5.17 μM EC_{50} for 6-azauridine reported here, so the potential usefulness in treating SOSV even at lower and less frequent doses should be further evaluated. 2′-dFC has been shown to potently inhibit several other negative strand viruses, including influenza and hepatitis C virus [37,38], although concerns over mitochondrial toxicity have limited the therapeutic use of 2′-dFC and its derivatives to date [39]. However, the potent antiviral activity of 2′-dFC makes worthwhile to investigate whether other 2′-deoxynucleoside analogs have similar antiviral activity against SOSV in the absence of toxicity.

The antiviral activity demonstrated by ribavirin was expected, and has been reported previously for NiV [22,40,41]. Ribavirin has also been used to treat human patients during a non-randomized, unblinded limited clinical trial during an NiV outbreak in Malaysia in 1998–

Table 1. Selected compounds' 50% effective concentrations (EC_{50}), 50% cytotoxic concentrations (CC_{50}), and selectivity indices (SI) determined by minigenome and reporter virus screening assays.

Compound	Minigenome Screen		rSOSV/ZsG Screen		CC_{50}	Compound Class
	EC_{50}	SI	EC_{50}	SI		
Ribavirin	5.91 ± 0.85	> 8	6.10 ± 0.09	> 8	> 50.0	Nucleoside analog
2′-deoxy-2′-fluorocytidine	1.31 ± 0.15	> 38	1.48 ± 0.22	> 33	> 50.0	Nucleoside analog
5-fluorouridine	0.29 ± 0.13	> 172	NT	NT	> 50.0	Nucleoside analog
Mycophenolic acid	± 0.06	7	0.33 ± 0.04	5	1.74 ± 0.42	IMPDH inhibitor
6-azauridine	5.17 ± 1.01	> 9	7.99 ± 1.32	> 6	> 50.0	Nucleoside analog
09167	NT	NT	0.67 ± 0.05	> 74	>50.0	Innate immune antagonist

NT, not tested; IMPDH, inosine monophosphate dehydrogenase. All values in μM ± standard deviation from at least 3 independent experiments.
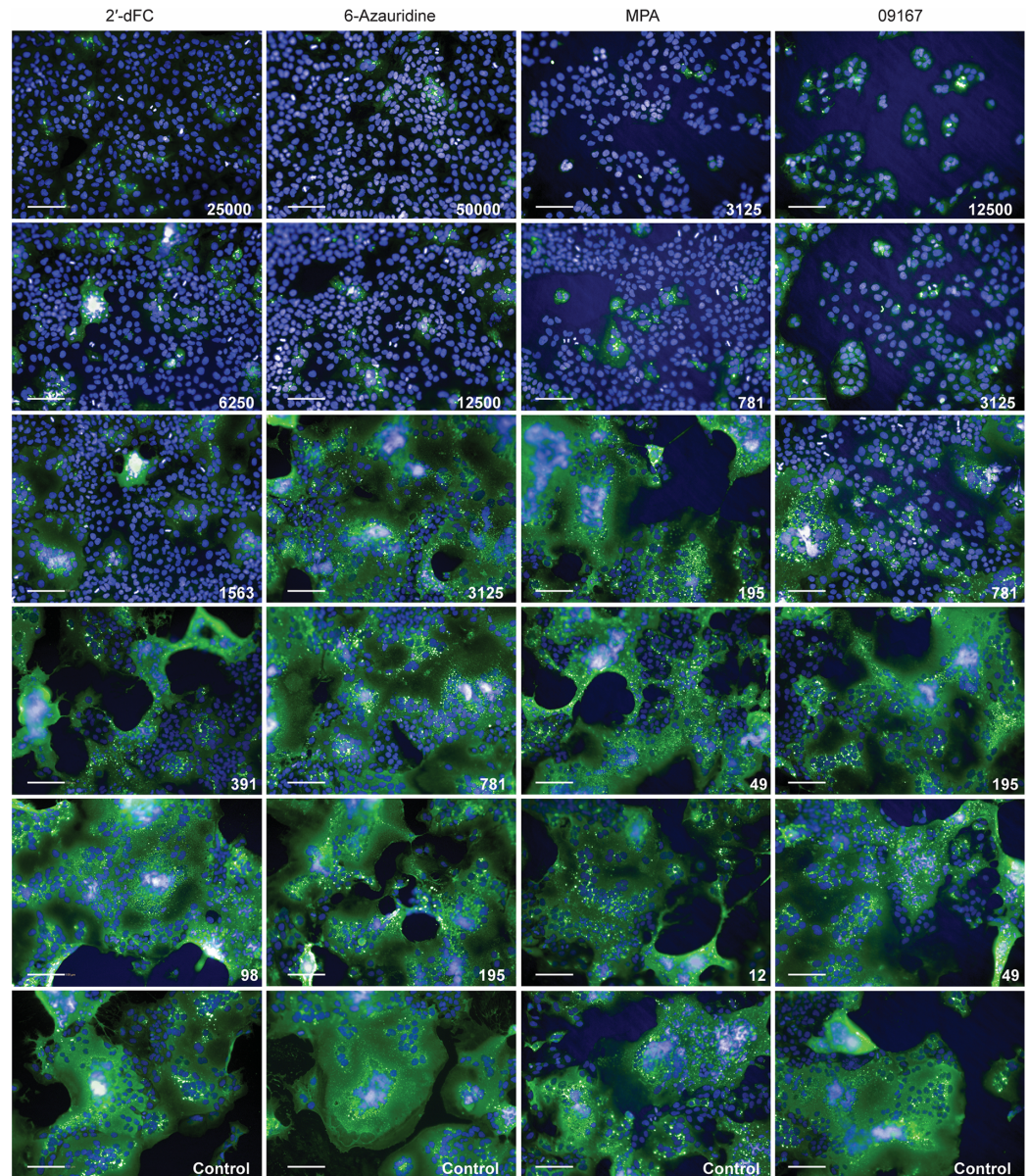
Fig 5. Immunofluorescent imaging of rSOSV infected Huh7 cells treated with selected antiviral compounds. Huh7 cells were treated with serial dilutions of either 2′-deoxy-2′-fluorocytidine (2′-dFC), 6-azauridine, mycophenolic acid (MPA), or 09167 1 h prior to infection with rSOSV at MOI 0.2. At 48 hpi, cells were fixed and SOSV proteins (green) and cell nuclei (blue) visualized by immunofluorescence. Concentration of compound is shown in white text on each representative image (mM); control cells were treated with DMSO only. Images taken using a 20 × objective. White bar represents 100 μm.

https://doi.org/10.1371/journal.pntd.0006326.g005

1999; mortality was reduced by 37% in the treated group [42]. However, its effectiveness when used in NiV animal models is less clear [40,43,44]. A similar discrepancy between in vivo and in vitro potency of these compounds may exist for SOSV, although this will remain unclear until a suitable SOSV animal model is developed. Promisingly, the limiting factor to henipa-virus treatment effectiveness appears to be the compound's ability to cross the blood-brain bar-rier (BBB). Ribavirin treatment in a non-human primate model of HeV infection reduced viral loads to levels low enough to prevent development of the respiratory signs of infection, but not

to prevent spread to the central nervous system [44]. As ribavirin cannot cross the BBB, the disease then manifested as neurological signs. However, no neurological symptoms were reported from the one SOSV case to date, so nucleoside analogs such as ribavirin, 6-azauridine, and 2′-dFC may be more effective treatment options for this disease.

In conclusion, we have developed a minigenome assay to investigate SOSV replication and transcriptional processes, as well as a rescue system to recover infectious recombinant virus. We used this system to rescue a recombinant SOSV capable of expressing a fluorescent reporter in infected cells with no loss of fitness compared to parental virus. A high-throughput screen using both systems identified 3 compounds that inhibited SOSV replication with acceptable SI values, providing information that may help direct therapeutic options for any future cases of SOSV. Finally, as well as being a powerful tool for analyzing mechanisms of SOSV pathogenesis, the minigenome and reporter systems may help us better understand the potential public health threats posed by bat-transmitted paramyxoviruses, and provide strategies on best combating these emerging threats.

Supporting information

S1 Fig. Plasmids use in the SOSV minigenome assay. The SOSV minigenome (mg) segment, containing the SOSV leader sequence and gene start for the nucleoprotein ORF, the ZsGreen1 ORF (ZsG), the polymerase ORF gene end, and the SOSV trailer sequence (Genbank #MG880223). Expression is controlled RNA-polymerase I promoter (pol I prom) and a RNA-polymerase I terminator sequences (pol I term).
(TIF)

S2 Fig. Plasmids used in the rescue of rSOSV (pSOSV FL) and rSOSV/ZsG (pSOSV/ZsG FL). Red arrows represent full-length viral genome, blue arrows represent viral protein open reading frames: NP–nucleoprotein; P–phosphoprotein; V–V protein; M–matrix protein; F–fusion protein; HN–hemagglutinin-neuraminidase; L–polymerase. Green arrow represents ZsGreen1 (ZsG) open reading frame. T7 prom–T7 polymerase promoter; HDV Rz–Hepatitis D virus ribozyme; T7term–T7 polymerase terminator; P2A –nucleotide sequence encoding the self-cleaving amino acid motif from porcine teschovirus 1. Sequences available at: pSOSV FL, Genbank #MG880224; pSOSV/ZsG FL, Genbank #MG880225).
(TIF)

S1 Table. Screening a panel of selected compounds for inhibition of SOSV minigenome in Huh7 cells. Compounds were screened for activity at concentrations of 5000, 500, and 50 nM, with cell viability determined concurrently by assessing ATP content.
(DOCX)

Acknowledgments

Author Contributions

Conceptualization: Stephen R. Welch, Ayan K. Chakrabarti, Michael K. Lo, Christina F. Spiropoulou, César G. Albariño.

Formal analysis: Stephen R. Welch, Michael K. Lo, César G. Albariño.

References

1. Lamb RA, Parks GD. Paramyxoviridae. Knipe DM, Howley PM, Cohen JI, Griffin DE, Lamb RA, Martin MA et al. Fields Virology. Lippincott Williams & Wilkins: Philadelphia, PA, USA; 2013;

2. Hollinger FB, Pavri KM. Bat parainfluenza virus. Immunological, chemical, and physical properties. Am J Trop Med Hyg. 1971; 20: 131–8. Available: http://www.ncbi.nlm.nih.gov/pubmed/4327914 PMID: 4327914

3. Wong S, Lau S, Woo P, Yue K-Y. Bats as a continuing source of emerging infections in humans. Rev Med Virol. 2007; 17: 67–91. Available: http://www.ncbi.nlm.nih.gov/pubmed/17042030 https://doi.org/10.1002/rmv.520 PMID: 17042030

4. Pavri KM, Singh KR, Hollinger FB. Isolation of a new parainfluenza virus from a frugivorous bat, Rousettus leschenaulti, collected at Poona, India. Am J Trop Med Hyg. 1971; 20: 125–30. Available: http://www.ncbi.nlm.nih.gov/pubmed/4327913 PMID: 4327913

5. Middleton DJ, Weingartl HM. Henipaviruses in their natural animal hosts. Curr Top Microbiol Immunol. 2012; 359: 105–21. Available: http://www.ncbi.nlm.nih.gov/pubmed/22476529 https://doi.org/10.1007/82_2012_210 PMID: 22476529

6. Murray K, Selleck P, Hooper P, Hyatt A, Gould A, Gleeson L, et al. A morbillivirus that caused fatal disease in horses and humans. Science. 1995; 268: 94–7. Available: http://www.ncbi.nlm.nih.gov/pubmed/7701348 PMID: 7701348

7. Field HE. Hendra virus ecology and transmission. Curr Opin Virol. 2016; 16: 120–125. Available: http://www.ncbi.nlm.nih.gov/pubmed/26978066 https://doi.org/10.1016/j.coviro.2016.02.004 PMID: 26978066

8. Clayton BA. Nipah virus: transmission of a zoonotic paramyxovirus. Curr Opin Virol. 2017; 22: 97–104. Available: http://www.ncbi.nlm.nih.gov/pubmed/28088124 https://doi.org/10.1016/j.coviro.2016.12.003 PMID: 28088124

9. ICTV. International Committee on Taxonomy of Viruses (ICTV) [WWW Document], n.d. Int. Comm. Taxon. Viruses ICTV. [Internet]. 2017. Available: https://talk.ictvonline.org/taxonomy/p/taxonomy-history?taxnode_id=20165119

10. Albariño CG, Foltzer M, Towner JS, Rowe LA, Campbell S, Jaramillo CM, et al. Novel paramyxovirus associated with severe acute febrile disease, South Sudan and Uganda, 2012. Emerg Infect Dis. 2014; 20: 211–6. Available: http://www.ncbi.nlm.nih.gov/pubmed/24447466 https://doi.org/10.3201/eid2002.131620 PMID: 24447466

11. Amman BR, Albariño CG, Bird BH, Nyakarahuka L, Sealy TK, Balinandi S, et al. A Recently Discovered Pathogenic Paramyxovirus, Sosuga Virus, is Present in Rousettus aegyptiacus Fruit Bats at Multiple Locations in Uganda. J Wildl Dis. 2015; 51: 774–9. Available: http://www.ncbi.nlm.nih.gov/pubmed/25919464 https://doi.org/10.7589/2015-02-044 PMID: 25919464

12. Reed LJ, Muench H. A simple method for estimating fifty percent endpoints. Am J Epidemiol. 1938; 27: 493–497. Available: https://doi.org/10.1093/oxfordjournals.aje.a118408

13. Zhang, Chung, Oldenburg. A Simple Statistical Parameter for Use in Evaluation and Validation of High Throughput Screening Assays. J Biomol Screen. 1999; 4: 67–73. Available: http://www.ncbi.nlm.nih.gov/pubmed/10838414 https://doi.org/10.1177/108705719900400206 PMID: 10838414

14. Mohr EL, McMullan LK, Lo MK, Spengler JR, Bergeron É, Albariño CG, et al. Inhibitors of cellular kinases with broad-spectrum antiviral activity for hemorrhagic fever viruses. Antiviral Res. Elsevier B.V.; 2015; 120: 40–7. Available: http://www.ncbi.nlm.nih.gov/pubmed/25986249

15. Welch SR, Guerrero LW, Chakrabarti AK, McMullan LK, Flint M, Bluemling GR, et al. Lassa and Ebola virus inhibitors identified using minigenome and recombinant virus reporter systems. Antiviral Res. 2016; 136: 9–18. Available: http://www.ncbi.nlm.nih.gov/pubmed/27771389 https://doi.org/10.1016/j.antiviral.2016.10.007 PMID: 27771389

16. Welch SR, Scholte FEMM, Flint M, Chatterjee P, Nichol ST, Bergeron É, et al. Identification of 2'-deoxy-2'-fluorocytidine as a potent inhibitor of Crimean-Congo hemorrhagic fever virus replication using a recombinant fluorescent reporter virus. Antiviral Res. Elsevier; 2017; 147: 91–99. Available: http://www.ncbi.nlm.nih.gov/pubmed/29024765 https://doi.org/10.1016/j.antiviral.2017.10.008 PMID: 29024765

17. Lo MK, Jordan R, Arvey A, Sudhamsu J, Shrivastava-Ranjan P, Hotard AL, et al. GS-5734 and its parent nucleoside analog inhibit Filo-, Pneumo-, and Paramyxoviruses. Sci Rep. 2017; 7: 43395. Available: http://www.ncbi.nlm.nih.gov/pubmed/28262699 https://doi.org/10.1038/srep43395 PMID: 28262699

18. Park A, Yun T, Hill TE, Ikegami T, Juelich TL, Smith JK, et al. Optimized P2A for reporter gene insertion into Nipah virus results in efficient ribosomal skipping and wild-type lethality. J Gen Virol. 2016; 97: 839–43. Available: http://www.ncbi.nlm.nih.gov/pubmed/26781134 https://doi.org/10.1099/jgv.0.000405 PMID: 26781134

19. Yun T, Park A, Hill TE, Pernet O, Beaty SM, Juelich TL, et al. Efficient reverse genetics reveals genetic determinants of budding and fusogenic differences between Nipah and Hendra viruses and enables real-time monitoring of viral spread in small animal models of henipavirus infection. J Virol. 2015; 89: 1242–53. Available: http://www.ncbi.nlm.nih.gov/pubmed/25392218 https://doi.org/10.1128/JVI.02583-14 PMID: 25392218

20. Yoneda M, Guillaume V, Ikeda F, Sakuma Y, Sato H, Wild TF, et al. Establishment of a Nipah virus rescue system. Proc Natl Acad Sci U S A. 2006; 103: 16508–13. Available: http://www.ncbi.nlm.nih.gov/pubmed/17053073 https://doi.org/10.1073/pnas.0606972103 PMID: 17053073

21. Marsh GA, Virtue ER, Smith I, Todd S, Arkinstall R, Frazer L, et al. Recombinant Hendra viruses expressing a reporter gene retain pathogenicity in ferrets. Virol J. 2013; 10: 95. Available: http://www.ncbi.nlm.nih.gov/pubmed/23521919 https://doi.org/10.1186/1743-422X-10-95 PMID: 23521919

22. Lo MK, Nichol ST, Spiropoulou CF. Evaluation of luciferase and GFP-expressing Nipah viruses for rapid quantitative antiviral screening. Antivir Res. 2014; 106: 53–60. Available: http://www.ncbi.nlm.nih.gov/pubmed/24680955 https://doi.org/10.1016/j.antiviral.2014.03.011 PMID: 24680955

23. Kim JH, Lee SR, Li LH, Park HJ, Park JH, Lee KY, et al. High cleavage efficiency of a 2A peptide derived from porcine teschovirus-1 in human cell lines, zebrafish and mice. PLoS One. 2011; 6: e18556. Available: http://www.ncbi.nlm.nih.gov/pubmed/21602908 https://doi.org/10.1371/journal.pone.0018556 PMID: 21602908

24. Yan D, Krumm SA, Sun A, Steinhauer DA, Luo M, Moore ML, et al. Dual myxovirus screen identifies a small-molecule agonist of the host antiviral response. J Virol. 2013; 87: 11076–87. Available: http://www.ncbi.nlm.nih.gov/pubmed/23926334 https://doi.org/10.1128/JVI.01425-13 PMID: 23926334

25. Chant K, Chan R, Smith M, Dwyer DE, Kirkland P. Probable human infection with a newly described virus in the family Paramyxoviridae. The NSW Expert Group. Emerg Infect Dis. 2009; 4: 273–5. Available: http://www.ncbi.nlm.nih.gov/pubmed/9621198

26. Zeltina A, Bowden TA, Lee B. Emerging Paramyxoviruses: Receptor Tropism and Zoonotic Potential. PLoS Pathog. 2016; 12: e1005390. Available: http://www.ncbi.nlm.nih.gov/pubmed/26915013 https://doi.org/10.1371/journal.ppat.1005390 PMID: 26915013

27. Thibault PA, Watkinson RE, Moreira-Soto A, Drexler JF, Lee B. Zoonotic Potential of Emerging Paramyxoviruses: Knowns and Unknowns. Adv Virus Res. United States; 2017; 98: 1–55. https://doi.org/10.1016/bs.aivir.2016.12.001 PMID: 28433050

28. Drexler JF, Corman VM, Müller MA, Maganga GD, Vallo P, Binger T, et al. Bats host major mammalian paramyxoviruses. Nat Commun. England; 2012; 3: 796. Available: http://www.ncbi.nlm.nih.gov/pubmed/22531181 https://doi.org/10.1038/ncomms1796 PMID: 22531181

29. Freiberg A, Dolores LK, Enterlein S, Flick R. Establishment and characterization of plasmid-driven mini-genome rescue systems for Nipah virus: RNA polymerase I- and T7-catalyzed generation of functional paramyxoviral RNA. Virology. 2008; 370: 33–44. Available: http://www.ncbi.nlm.nih.gov/pubmed/17904180 https://doi.org/10.1016/j.virol.2007.08.008 PMID: 17904180

30. Hashimoto K, Ono N, Tatsuo H, Minagawa H, Takeda M, Takeuchi K, et al. SLAM (CD150)-independent measles virus entry as revealed by recombinant virus expressing green fluorescent protein. J Virol. 2002; 76: 6743–9. Available: http://www.ncbi.nlm.nih.gov/pubmed/12050387 https://doi.org/10.1128/JVI.76.13.6743-6749.2002 PMID: 12050387

31. Burke CW, Mason JN, Surman SL, Jones BG, Dalloneau E, Hurwitz JL, et al. Illumination of parainfluenza virus infection and transmission in living animals reveals a tissue-specific dichotomy. PLoS Pathog. 2011; 7: e1002134. Available: http://www.ncbi.nlm.nih.gov/pubmed/21750677 https://doi.org/10.1371/journal.ppat.1002134 PMID: 21750677

32. Hosoya M, Shigeta S, Nakamura K, De Clercq E. Inhibitory effect of selected antiviral compounds on measles (SSPE) virus replication in vitro. Antiviral Res. 1989; 12: 87–97. Available: http://www.ncbi.nlm.nih.gov/pubmed/2480744 PMID: 2480744

33. Roth JP, Li JK-K, Smee DF, Morrey JD, Barnard DL. A recombinant, infectious human parainfluenza virus type 3 expressing the enhanced green fluorescent protein for use in high-throughput antiviral assays. Antiviral Res. 2009; 82: 12–21. Available: http://www.ncbi.nlm.nih.gov/pubmed/19189850 https://doi.org/10.1016/j.antiviral.2009.01.001 PMID: 19189850

34. Deneau DG, Farber EM. The treatment of psoriasis with azaribine. Dermatologica. 1975; 151: 158–63. Available: http://www.ncbi.nlm.nih.gov/pubmed/1243822 PMID: 1243822

35. Crutcher WA, Moschella SL. Double-blind controlled crossover high-dose study of Azaribine in psoriasis. Br J Dermatol. 1975; 92: 199–205. Available: http://www.ncbi.nlm.nih.gov/pubmed/1096923 PMID: 1096923

36. Creasy WA, Fink ME, Handschumacher RE, Calabresi P. Clinical and pharmacological studies with 2',3',5'-triacetyl-6-azauridine. Cancer Res. 1963; 23: 444–53. Available: http://www.ncbi.nlm.nih.gov/pubmed/14023746 PMID: 14023746

37. Kumaki Y, Day CW, Smee DF, Morrey JD, Barnard DL. In vitro and in vivo efficacy of fluorodeoxycytidine analogs against highly pathogenic avian influenza H5N1, seasonal, and pandemic H1N1 virus infections. Antiviral Res. 2011; 92: 329–40. Available: http://www.ncbi.nlm.nih.gov/pubmed/21925541 https://doi.org/10.1016/j.antiviral.2011.09.001 PMID: 21925541

38. Stuyver LJ, McBrayer TR, Whitaker T, Tharnish PM, Ramesh M, Lostia S, et al. Inhibition of the subgenomic hepatitis C virus replicon in huh-7 cells by 2'-deoxy-2'-fluorocytidine. Antimicrob Agents Chemother. 2004; 48: 651–4. Available: http://www.ncbi.nlm.nih.gov/pubmed/14742230 https://doi.org/10.1128/AAC.48.2.651-654.2004 PMID: 14742230

39. Arnold JJ, Sharma SD, Feng JY, Ray AS, Smidansky ED, Kireeva ML, et al. Sensitivity of mitochondrial transcription and resistance of RNA polymerase II dependent nuclear transcription to antiviral ribonucleosides. PLoS Pathog. 2012; 8: e1003030. Available: http://www.ncbi.nlm.nih.gov/pubmed/23166498 https://doi.org/10.1371/journal.ppat.1003030 PMID: 23166498

40. Georges-Courbot MC, Contamin H, Faure C, Loth P, Baize S, Leyssen P, et al. Poly(I)-Poly(C12U) but Not Ribavirin Prevents Death in a Hamster Model of Nipah Virus Infection. Antimicrob Agents Chemother. 2006; 50: 1768–1772. Available: http://www.ncbi.nlm.nih.gov/pubmed/16641448 https://doi.org/10.1128/AAC.50.5.1768-1772.2006 PMID: 16641448

41. Wright PJ, Crameri G, Eaton BT. RNA synthesis during infection by Hendra virus: an examination by quantitative real-time PCR of RNA accumulation, the effect of ribavirin and the attenuation of transcription. Arch Virol. 2005; 150: 521–32. Available: http://www.ncbi.nlm.nih.gov/pubmed/15526144 https://doi.org/10.1007/s00705-004-0417-5 PMID: 15526144

42. Chong HT, Kamarulzaman A, Tan CT, Goh KJ, Thayaparan T, Kunjapan SR, et al. Treatment of acute Nipah encephalitis with ribavirin. Ann Neurol. 2001; 49: 810–3. Available: http://www.ncbi.nlm.nih.gov/pubmed/11409437 PMID: 11409437

43. Freiberg AN, Worthy MN, Lee B, Holbrook MR. Combined chloroquine and ribavirin treatment does not prevent death in a hamster model of Nipah and Hendra virus infection. J Gen Virol. 2010; 91: 765–72. Available: http://www.ncbi.nlm.nih.gov/pubmed/19889926 https://doi.org/10.1099/vir.0.017269-0 PMID: 19889926

44. Rockx B, Bossart KN, Feldmann F, Geisbert JB, Hickey AC, Brining D, et al. A novel model of lethal Hendra virus infection in African green monkeys and the effectiveness of ribavirin treatment. J Virol. 2010; 84: 9831–9. Available: http://www.ncbi.nlm.nih.gov/pubmed/20660198 https://doi.org/10.1128/JVI.01163-10 PMID: 20660198